Coexistence of two states in optically homogeneous silica glass during the transformation in short-range order

Tomoko Sato,[1] Nobumasa Funamori,[2,3,4] Daisuke Wakabayashi,[2,3] Keisuke Nishida,[4] and Takumi Kikegawa[2,3]
[1]*Department of Earth and Planetary Systems Science, Hiroshima University, Higashi-Hiroshima 739-8526, Japan*
[2]*Institute of Materials Structure Science, High Energy Accelerator Research Organization (KEK), Tsukuba 305-0801, Japan*
[3]*Department of Materials Structure Science, Graduate University for Advanced Studies, Tsukuba 305-0801, Japan*
[4]*Department of Earth and Planetary Science, University of Tokyo, Tokyo 113-0033, Japan*

(Received 1 July 2018; published 18 October 2018)

Silica glass is an optically homogeneous material with many practical applications. Unlike crystalline materials, it remains optically homogeneous during transformations. However, high-pressure *in situ* small-angle x-ray-scattering measurements indicate an increase in the scattering intensity during the transformation in short-range order between fourfold-coordinated and sixfold-coordinated amorphous polymorphs, providing strong evidence for heterogeneity. Detailed analyses suggest that silica glass consists of optically invisible subnanometer-scale domains for the two amorphous polymorphs and boundary region between them. The boundary region, which likely has an intermediate structure, is comparable in size to the domains, and works as a buffer to prevent the glass from cracking during the transformation. The transformation is more drastic and the domains are more distinct upon decompression than compression.

DOI: 10.1103/PhysRevB.98.144111

I. INTRODUCTION

Polyamorphism has been studied intensively since Bridgman and Šimon [1] discovered the permanent-densification phenomenon in SiO_2 glass. However, many problems remain unsolved. One of the most mysterious is about the intermediate state of amorphous–amorphous transformations. When a single crystal transforms into a different phase, heterogeneous features such as grain boundaries and cracks emerge. These features, which can be observed by optical microscopy (or even the naked eye) [2], are attributed to the generation and growth of daughter-phase nuclei in mother-phase single crystals. By contrast, indications of heterogeneity are not detected in the case of glasses [3,4].

A good example is the pressure-induced transformation in short-range order of SiO_2 glass from the fourfold-coordinated structure to the sixfold-coordinated structure. This transformation is accompanied by a ∼30% increase in density [5–7]. Despite the large changes in the structure and the density, the glass remains optically homogeneous during the transformation. Why does it remain homogeneous? Does the glass change its structure continuously and homogeneously unlike crystals [8–10]? To answer these questions, the intermediate state of the transformation must be unveiled. X-ray diffraction is commonly used to study the intermediate state of a crystal, but it is not useful for glass because x-ray diffraction provides limited structural information such as the average interatomic distance and coordination number [11].

Small-angle x-ray scattering is a method that fills up the length scale between optical microscopy (micron scale) and x-ray diffraction (angstrom scale). It provides information about the sample's heterogeneity [12]. In fact, this method provided definitive evidence for the coexistence of two liquid phases during the first-order phase transformation in oxide liquids at ambient pressure [13] and that for the density fluctuation during the continuous phase transformation in chalcogen binary liquids at nearly ambient pressure [14]. Herein we develop small-angle x-ray-scattering techniques to study the heterogeneity of glass at high pressures, and apply them to unveil the intermediate state of the transformation in SiO_2 glass.

II. EXPERIMENTS

High-pressure *in situ* small-angle x-ray-scattering experiments for SiO_2 glass were conducted using a newly developed system at the BL-18C beamline of the Photon Factory (Tsukuba, Japan). A special setup, which differs from the ordinary one dedicated to x-ray diffraction, was prepared to measure x-ray scatterings in the low-Q range for samples in diamond-anvil high-pressure cells. An additional collimator was set between the sample and the x-ray shaping collimator to remove scattering from the shaping collimator. A vacuum chamber was installed downstream of the sample to remove scattering due to air. An imaging plate was used in the vacuum chamber to measure the scatterings from the sample in the Q range from 0.14 to 4.0 $Å^{-1}$ simultaneously. To accurately determine the scattering intensity from the sample, we used the following settings. The x-ray energy was set to 15.3 keV, considering the x-ray absorption and glitches of the anvils [15,16]. Because the signal increases with sample thickness, a c-BN gasket was used instead of an ordinary metal gasket [17]. The measurements were conducted with a NaCl pressure medium during the compression process up to 40 GPa and the subsequent decompression process down to ambient pressure at room temperature. We also conducted optical-microscope observations with a rhenium gasket and a NaCl pressure medium in a separate run from the

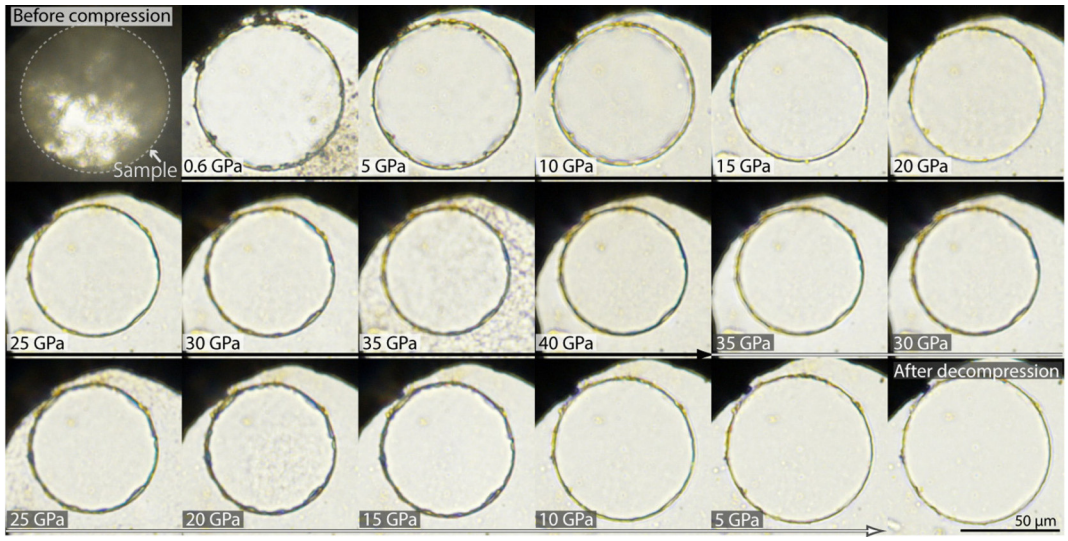

FIG. 1. Optical-microscope pictures of SiO_2 glass in a diamond-anvil cell with a NaCl pressure medium. The black area is the gasket. The arrow shows the time series of the experiment. Black and white denote pressures upon compression and decompression, respectively. Heterogeneity is not observed in the sample at all pressures. The sample chamber is initially opaque because the grain boundaries of NaCl do not stick to each other. The chamber becomes slightly heterogeneous at 35 GPa upon compression and 20 GPa upon decompression due to the phase transformation of NaCl [18]. The sample diameter is larger after decompression than before compression due to the plastic deformation [4].

small-angle x-ray-scattering experiments, to demonstrate the optical homogeneity during the transformation between the fourfold-coordinated structure and the sixfold-coordinated structure.

III. RESULTS AND DISCUSSION

A. Optical-microscope observations and small-angle x-ray-scattering measurements

Figure 1 shows the optical-microscope photographs of SiO_2 glass at high pressures. Heterogeneity is not observed (Fig. 1). Only the sample size changes significantly. The sample chamber is initially opaque due to the difference in the refractive index between the NaCl particles and surrounding air before the compression, but becomes transparent in the subsequent compression and decompression processes. Similarly, the difference in density between NaCl and air affects the small-angle x-ray-scattering data at ambient pressure before compression, but the effect becomes very small and can be neglected in subsequent measurements after grain boundaries stick to each other by compression [19].

Figure 2 shows the x-ray-scattering patterns of SiO_2 glass at high pressures. Figure 3 shows the pressure dependence of the position and the height of the first sharp diffraction peak (FSDP) and I_{av}, which is defined as the scattering intensity averaged over the low-Q range between 0.14 and 0.60 $Å^{-1}$. Upon compression, the position and the height of the FSDP change monotonically with pressure, whereas I_{av} shows a maximum at ∼25 GPa. The tail of the FSDP extends to the low-Q range upon compression to 10 GPa. Consequently, the low-Q scattering intensity upon compression below 10 GPa (gray symbols in Fig. 3) is not discussed. Upon decompression, the position and the height of the FSDP change drastically between 15 and 10 GPa. This is accompanied by a more obvious maximum in I_{av}. The pressure dependence of the position of the FSDP (Fig. 3) is consistent with available data [19,23].

Since the transformation from the fourfold-coordinated structure to the sixfold-coordinated structure occurs mainly between 20 and 35 GPa [5,6,9,10,24–27], it is conceivable that the maximum of I_{av} upon compression is due to this transformation. Although fewer studies examine the behavior of SiO_2 glass upon decompression compared to that upon compression, the sixfold-coordinated structure reverts back to the fourfold-coordinated structure (the fully densified fourfold-coordinated structure [28,29]) below ∼20 GPa [9,23,25]. Therefore, the drastic change observed upon decompression is attributed to the transformation from the sixfold-coordinated structure to the fourfold-coordinated structure. The increase in the intensity of the small-angle x-ray scattering provides definitive evidence of a heterogeneous intermediate state during the transformation [12].

B. Analyses with two-phase mixing model

The following procedure was used to analyze the small-angle x-ray-scattering data. Since the scattering intensity in the low-Q range is the Fourier transform of the autocorrelation function of electron density distribution [12], more detailed information about the heterogeneity such as the degree and scale of variation during the transformation can be derived from the pattern. By extending the two-phase mixing model proposed by Debye and Beuche [30] to the case of an unsharp domain boundary, the low-Q scattering intensity is described as [19]

$$I(Q) = \frac{I_0}{(1+\xi^2 Q^2)^2} H(Q)^2 + I_{\text{intr}}. \quad (1)$$

Here, $I(Q)$ and ξ represent the scattering intensity from an average atom and half the correlation length, respectively.

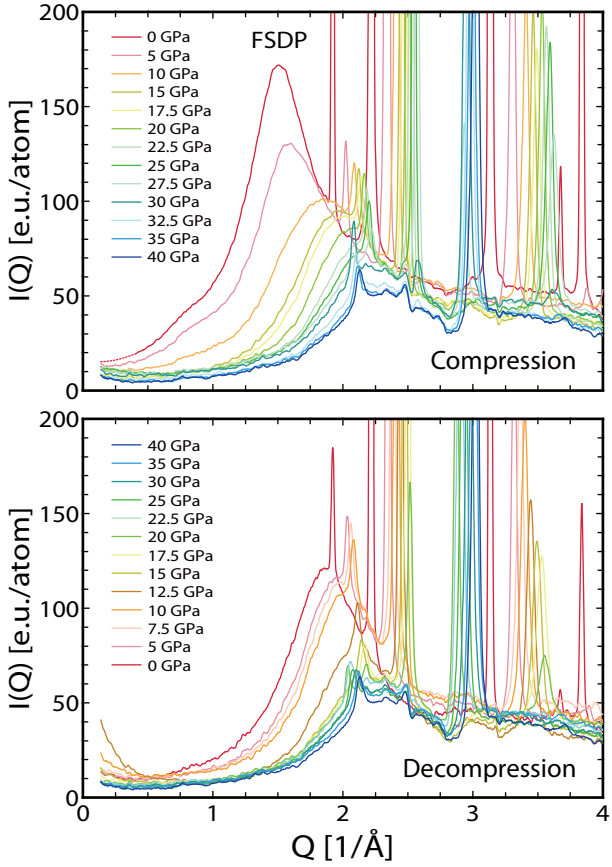

FIG. 2. X-ray-scattering patterns of SiO_2 glass under high pressure. Sharp peaks at $Q > \sim 2\,\text{Å}^{-1}$ are from the NaCl pressure medium. Upon compression, the tail of the FSDP extends to the low-Q range ($Q < \sim 0.6\,\text{Å}^{-1}$) at 0–10 GPa. At ambient pressure before compression, $I(Q)$ at $Q < \sim 0.4\,\text{Å}^{-1}$ cannot be measured due to the intense scatterings from grain boundaries of NaCl. (The red dotted line is just an expectation.) The position and the height of the FSDP after decompression differ from those before compression due to the permanent densification [28,29].

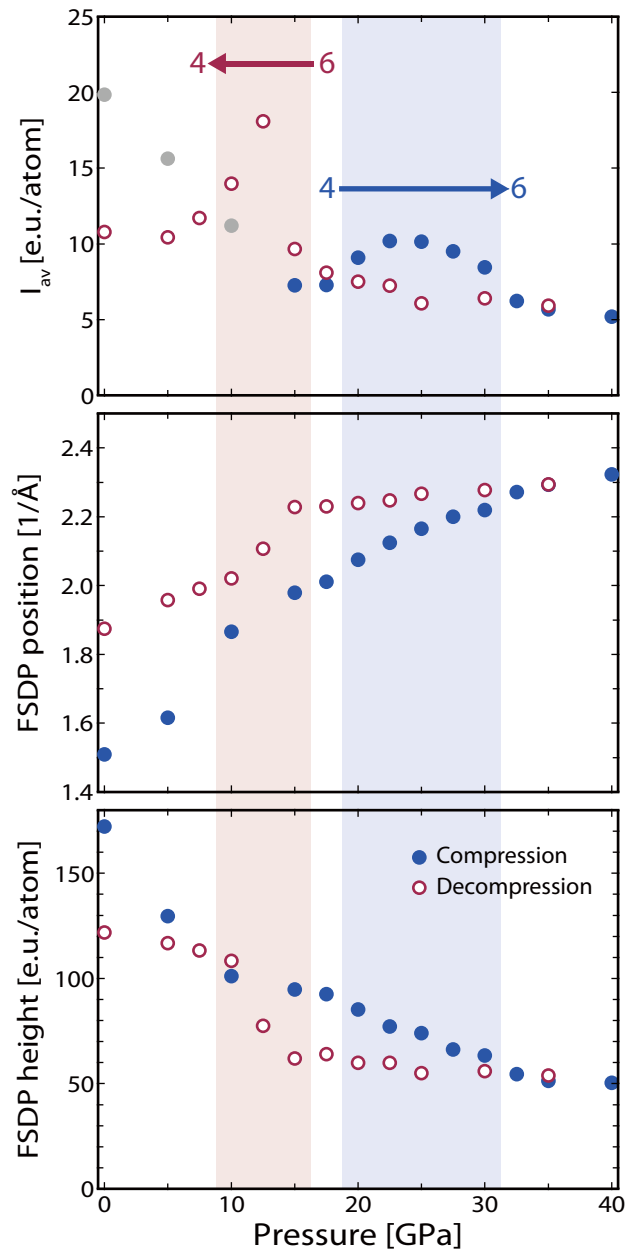

FIG. 3. Pressure dependence of I_{av}, the average scattering intensity in the low-Q range from 0.14 to 0.60 Å^{-1}, and the position and the height of the FSDP. Solid and open symbols represent the data upon compression and decompression, respectively. Gray symbols for I_{av} denote the data upon compression affected by the tail of the FSDP.

I_{intr} represents the scattering intensity due to the intrinsic density fluctuation inherited from a liquid state (or a supercooled liquid state). $H(Q)$ is the Fourier transform of the one-dimensional form of the smoothing function $h(\mathbf{r})$. Considering an unsharp boundary where the density changes linearly within the width E, $h(r)$ can be written as [31,32]

$$h(r) = \begin{cases} 1/E & |r| < E/2 \\ 0 & |r| > E/2 \end{cases}. \tag{2}$$

Then [19],

$$I_0 = 8\pi\xi^3 V \Delta\rho^2 \phi(1-\phi)\left(1 - \frac{2E}{3\xi}\right), \tag{3}$$

$$H(Q) = \frac{2}{EQ}\sin\left(\frac{EQ}{2}\right), \tag{4}$$

where $\Delta\rho$, ϕ, and V represent the difference in the electron density between the two phases, the volume fraction of one phase, and the volume occupied by an average atom, respectively. In Eq. (3), $8\pi\xi^3$ is a measure of the domain volume (including the boundary region) [12,19].

Equations (1)–(4) were fit to the scattering pattern at 12.5 GPa upon decompression, which has the most prominent increase in the low-Q scattering intensity. Based on the position and the height of the FSDP as well as the equations of state for the two relevant structures, i.e., the sixfold-coordinated and the fully densified fourfold-coordinated structures [5,29], $\phi = 0.5$ and the density difference of $1.0\,\text{g/cm}^3$ were assumed. At ambient pressure, I_{intr} of SiO_2

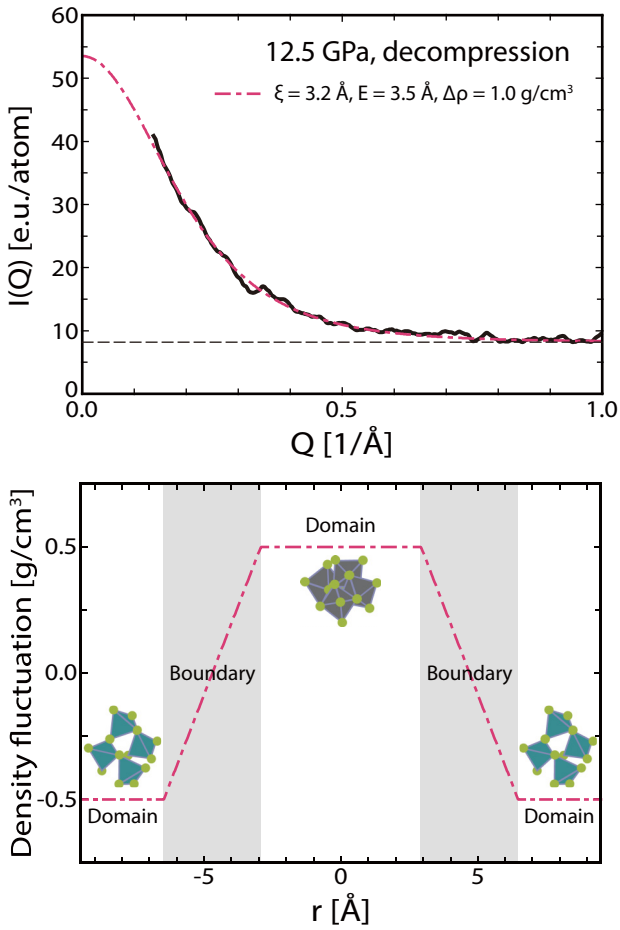

FIG. 4. Low-Q x-ray-scattering pattern of SiO_2 glass at 12.5 GPa upon decompression and the density-fluctuation model with a domain size of $[(8\pi\xi^3)^{1/3} - E]$ [12,19]. Red dash-dotted lines represent the fitting result with Eqs. (1)–(4). The thin dashed line corresponds to $I_{\rm intr}$, which is the scattering intensity due to the density fluctuation inherited from the liquid state. $\Delta\rho$ represents the difference in density in this figure, while it represents the difference in electron density elsewhere. The double of $(8\pi\xi^3)^{1/3}$ is ∼20 Å and this value corresponds to $Q = \sim 0.3$ Å^{-1}.

glass is ∼10 e.u./atom [33]. The scattering intensity of 1 e.u. corresponds to the classical scattering from a single electron [11,19]. At high pressures, $I_{\rm intr}$ is estimated to be 5–10 e.u./atom. (See the baseline of $I_{\rm av}$ in Fig. 3.) The analysis assumes that $I_{\rm intr}$ is equal to the intensity at $Q = \sim 1.0$ Å^{-1} (Fig. 4). The fitting indicates that I_0, ξ, and E are 45 e.u./atom, 3.2 Å, and 3.5 Å, respectively. The patterns at 15 and 10 GPa upon decompression can be well reproduced with $\phi = 0.05$ and 0.89 ($I_0 = 8.4$ and 18 e.u./atom), respectively, by assuming the same ξ and E as those at 12.5 GPa ($\xi = 3.2$ Å and $E = 3.5$ Å).

Figure 4 shows the one-dimensional density-fluctuation model with these parameters. The estimated domain size is ∼6 Å. Considering that the Si-O bond length is 1.6–1.7 Å both in the fourfold-coordinated structure and the sixfold-coordinated structure [5,10,24,25,27], several SiO_4 tetrahedrons and SiO_6 octahedrons likely form the fourfold-coordinated domain and the sixfold-coordinated domain, respectively, during the transformation. The structure in the boundary region may be classified as a fivefold-coordinated structure. The fraction of the fivefold-coordinated structure may be rather large because the boundary width is comparable to the domain size. Molecular-dynamics simulations predicted that fourfold-, fivefold-, and sixfold-coordinated silicon ions coexist during the transformation and the fraction of the fivefold-coordinated ions becomes rather large [34–37]. Our results are consistent with these predictions. However, larger-scale first-principle simulations may be necessary for detailed comparison with experiments.

The one-dimensional density-fluctuation model obtained by small-angle x-ray scattering (Fig. 4) well explains the lack of heterogeneous features such as grain boundaries and cracks in optical microscopy (Fig. 1), although the two structures coexist in SiO_2 glass during the transformation. First, optical microscopy cannot identify domains that are smaller than the wavelength of visible light. Second, the broad boundary region with an intermediate structure likely works as a buffer. It compensates for the large difference between the two structures, preventing the glass from cracking. The large boundary width, which is comparable to the domain size, highlights the difference from crystals displaying heterogeneous features during phase transformations.

C. Domain size and sluggishness of transformation

Compared to decompression, the transformation is sluggish and not prominent upon compression. I_0 is estimated to be $< \sim 10$ e.u./atom at 25 GPa upon compression (Figs. 2 and 3), which is much smaller than 45 e.u./atom at 12.5 GPa upon decompression. Based on the equations of state [5,29], the density difference between the sixfold-coordinated structure and the fully densified fourfold-coordinated structure is ∼0.88 g/cm^3 at 25 GPa. This corresponds to $I_0 = \sim 35$ e.u./atom, assuming the density is only difference between compression and decompression. This assumption is obviously incorrect because $I_0 < \sim 10$ e.u./atom. Unfortunately, it is difficult to determine the parameters by fitting. Nevertheless, according to Eq. (3), the difference in I_0 can be explained if ξ is smaller (∼2.6 Å assuming the same E and ∼2.0 Å assuming the same E/ξ), suggesting that domains are less distinct during compression than decompression. In the model proposed by Brazhkin and Lyapin [38], the sluggishness (pressure width) of a transformation and domain size are inversely correlated because the distribution of the Gibbs free energy of domains becomes broader as the domain size becomes smaller. Our observations and interpretations are also consistent with this model.

The difference between compression and decompression may be due to the variation in the intrinsic inhomogeneity of the fourfold-coordinated structure and the sixfold-coordinated structure. $I_{\rm intr}$ of the fourfold-coordinated structure is larger than that of the sixfold-coordinated structure. (See the baseline of $I_{\rm av}$ in Fig. 3.) Because the fourfold-coordinated structure has a larger inhomogeneity than the sixfold-coordinated structure, the nucleation of the sixfold-coordinated structure in the fourfold-coordinated structure may be easier than that of the fourfold-coordinated structure in the sixfold-coordinated structure. If this is the case, the transformation starts earlier

and proceeds more sluggishly upon compression than decompression. Therefore, the domain size becomes small upon compression and large upon decompression [38].

IV. CONCLUDING REMARKS

In this study, we obtained definitive experimental evidence for a heterogeneous intermediate state during the transformation of SiO_2 glass between the fourfold-coordinated structure and the sixfold-coordinated structure by high-pressure *in situ* small-angle x-ray-scattering measurements. Although the glass seems to change its structure continuously and homogeneously (Fig. 1), small domains of the two structures coexist with the broad boundary region, which works as a buffer composed of an intermediate structure (Fig. 4). The transformation proceeds heterogeneously by changing the ratio of the two structures.

In closing, we have two remarks. First, the view presented in the preceding paragraph may be applicable to other amorphous–amorphous transformations. For example, previous studies reported a similarity between GeO_2 glass and SiO_2 glass. The density change with pressure during the transformation in GeO_2 glass between the fourfold-coordinated structure and the sixfold-coordinated structure can be explained by a two-phase mixing model [39]. A certain fraction of germanium ions has a fivefold-coordinated structure [40]. The transformation is more sluggish upon compression than upon decompression [41]. Such hysteresis was also reported in B_2O_3 glass [42]. Moreover, some samples of amorphous ice recovered to ambient pressure show an increased intensity in small-angle neutron scattering [43], although the interpretation of the data is debatable. The transformation of amorphous ice can be optically detected and occurs rapidly [38,44]. Second, we expect that high-pressure *in situ* small-angle x-ray-scattering measurements will be applied to many other amorphous materials. We have proposed a general picture of the intermediate state of amorphous–amorphous transformations. Analogous to crystals, however, the transformations of amorphous materials should vary widely. Further studies on various amorphous materials will significantly deepen the understanding of polyamorphism.

ACKNOWLEDGMENTS

The authors thank K. Watanabe, H. Takada, T. Hata, T. Yokoi, and Y. Shigeoka for experimental support. Synchrotron x-ray experiments were carried out at Photon Factory. This work was in part supported by Grants-in-Aid for Scientific Research (Japan).

[1] P. W. Bridgman and I. Šimon, Effects of very high pressures on glass, J. Appl. Phys. **24**, 405 (1953).

[2] *Handbook of Crystal Growth Vol. 1. Fundamentals, Part A. Thermodynamics and Kinetics*, edited by D. T. J. Hurle (North-Holland, Amsterdam, 1993).

[3] Q. Mei, S. Sinogeikin, G. Shen, S. Amin, C. J. Benmore, and K. Ding, High-pressure x-ray diffraction measurements on vitreous GeO_2 under hydrostatic conditions, Phys. Rev. B **81**, 174113 (2010).

[4] D. Wakabayashi, N. Funamori, and T. Sato, Enhanced plasticity of silica glass at high pressure, Phys. Rev. B **91**, 014106 (2015).

[5] T. Sato and N. Funamori, Sixfold-Coordinated Amorphous Polymorph of SiO_2 Under High Pressure, Phys. Rev. Lett. **101**, 255502 (2008).

[6] S. Petitgirard, W. J. Malfait, B. Journaux, I. E. Collings, E. S. Jennings, I. Blanchard, I. Kantor, A. Kurnosov, M. Cotte, T. Dane, M. Burghammer, and D. C. Rubie, SiO_2 Glass Density to Lower-Mantle Pressures, Phys. Rev. Lett. **119**, 215701 (2017).

[7] S. J. Tracy, S. J. Turneaure, and T. S. Duffy, *In situ* X-Ray Diffraction of Shock-Compressed Fused Silica, Phys. Rev. Lett. **120**, 135702 (2018).

[8] E. M. Stolper and T. J. Ahrens, On the nature of pressure-induced coordination changes in silicate melts and glasses, Geophys. Res. Lett. **14**, 1231 (1987).

[9] Q. Williams and R. Jeanloz, Spectroscopic evidence for pressure-induced coordination changes in silicate glasses and melts, Science **239**, 902 (1988).

[10] T. Sato and N. Funamori, High-pressure structural transformation of SiO_2 glass up to 100 GPa, Phys. Rev. B **82**, 184102 (2010).

[11] B. E. Warren, *X-Ray Diffraction* (Addison-Wesley, Reading, MA, 1969).

[12] *Small-Angle X-Ray Scattering*, edited by O. Glatter and O. Kratky (Academic, London, 1982).

[13] G. N. Greaves, M. C. Wilding, S. Fearn, D. Langstaff, F. Kargl, S. Cox, Q. Vu Van, O. Majérus, C. J. Benmore, R. Weber, C. M. Martin, and L. Hennet, Detection of first-order liquid/liquid phase transitions in yttrium oxide–aluminum oxide melts, Science **322**, 566 (2008).

[14] Y. Kajihara, M. Inui, K. Matsuda, T. Nagao, and K. Ohara, Density fluctuations at the continuous liquid-liquid phase transition in chalcogen systems, Phys. Rev. B **86**, 214202 (2012).

[15] A. V. Sapelkin and S. C. Bayliss, X-ray absorption spectroscopy under high pressures in diamond anvil cells, High Press. Res. **21**, 315 (2001).

[16] T. Sato and N. Funamori, High-pressure *in situ* density measurement of low-Z noncrystalline materials with a diamond-anvil cell by an x-ray absorption method, Rev. Sci. Instrum. **79**, 073906 (2008).

[17] N. Funamori and T. Sato, A cubic boron nitride gasket for diamond-anvil experiments, Rev. Sci. Instrum. **79**, 053903 (2008).

[18] W. A. Basset, T. Takahashi, H. K. Mao, and J. S. Weaver, Pressure-induced phase transformation in NaCl, J. Appl. Phys. **39**, 319 (1968).

[19] See Supplemental Material at http://link.aps.org/supplemental/10.1103/PhysRevB.98.144111 for detailed information on the experiments and models. Supplemental Material includes Refs. [20–22].

[20] H. K. Mao, P. M. Bell, J. W. Shaner, and D. J. Steinberg, Specific volume measurements of Cu, Mo, Pd, and Ag and calibration of the ruby R_1 fluorescence pressure gauge from 0.06 to 1 Mbar, J. Appl. Phys. **49**, 3276 (1978).

[21] Y. Inamura, Y. Katayama, W. Utsumi, and K. Funakoshi, Transformations in the Intermediate-Range Structure of SiO_2 Glass Under High Pressure and Temperature, Phys. Rev. Lett. **93**, 015501 (2004).

[22] P. Debye, H. R. Anderson, Jr., and H. Brumberger, Scattering by an inhomogeneous solid. II. The correlation function and its application, J. Appl. Phys. **28**, 679 (1957).

[23] T. Sato, N. Funamori, and T. Yagi, Differential strain and residual anisotropy in silica glass, J. Appl. Phys. **114**, 103509 (2013).

[24] C. Meade, R. J. Hemley, and H. K. Mao, High-Pressure X-Ray Diffraction of SiO_2 Glass, Phys. Rev. Lett. **69**, 1387 (1992).

[25] C. J. Benmore, E. Soignard, S. A. Amin, M. Guthrie, S. D. Shastri, P. L. Lee, and J. L. Yarger, Structural and topological changes in silica glass at pressure, Phys. Rev. B. **81**, 054105 (2010).

[26] M. Murakami and J. D. Bass, Spectroscopic Evidence for Ultrahigh-Pressure Polymorphism in SiO_2 Glass, Phys. Rev. Lett. **104**, 025504 (2010).

[27] C. Prescher, V. B. Prakapenka, J. Stefanski, S. Jahn, L. B. Skinner, and Y. Wang, Beyond sixfold coordinated Si in SiO_2 glass at ultrahigh pressures, Proc. Natl. Acad. Sci. USA **114**, 10041 (2017).

[28] S. Susman, K. J. Volin, D. L. Price, M. Grimsditch, J. P. Rino, R. K. Kalia, P. Vashishta, G. Gwanmesia, Y. Wang, and R. C. Liebermann, Intermediate-range order in permanently densified vitreous SiO_2: A neutron-diffraction and molecular-dynamics study, Phys. Rev. B **43**, 1194 (1991).

[29] D. Wakabayashi, N. Funamori, T. Sato, and T. Taniguchi, Compression behavior of densified SiO_2 glass, Phys. Rev. B **84**, 144103 (2011).

[30] P. Debye and A. M. Bueche, Scattering by an inhomogeneous solid, J. Appl. Phys. **20**, 518 (1949).

[31] W. Ruland, Small-angle scattering of two-phase systems: Determination and significance of systematic deviations from Porod's law, J. Appl. Cryst. **4**, 70 (1971).

[32] C. G. Vonk, Investigation of non-ideal two-phase polymer structures by small-angle x-ray scattering, J. Appl. Cryst. **6**, 81 (1973).

[33] A. C. Wright, Neutron scattering from vitreous silica. V. The structure of vitreous silica: What have we learned from 60 years of diffraction studies? J. Non-Cryst. Solids **179**, 84 (1994).

[34] M. Wu, Y. Liang, J.-Z. Jiang, and J. S. Tse, Structure and properties of dense silica glass, Sci. Rep. **2**, 398 (2012).

[35] F. Yuan and L. Huang, Brittle to ductile transition in densified silica glass, Sci. Rep. **4**, 5035 (2014).

[36] A. Zeidler, K. Wezka, R. F. Rowlands, D. A. J. Whittaker, P. S. Salmon, A. Polidori, J. W. E. Drewitt, S. Klotz, H. E. Fischer, M. C. Wilding, C. L. Bull, M. G. Tucker, and M. Wilson, High-Pressure Transformation of SiO_2 Glass from a Tetrahedral to an Octahedral Network: A Joint Approach Using Neutron Diffraction and Molecular Dynamics, Phys. Rev. Lett. **113**, 135501 (2014).

[37] P. Koziatek, J. L. Barrat, and D. Rodney, Short- and medium-range orders in as-quenched and deformed SiO_2 glasses: An atomistic study, J. Non-Cryst. Solids **414**, 7 (2015).

[38] V. V. Brazhkin and A. G. Lyapin, Two scenarios for phase-transformation in disordered media, JETP Lett. **78**, 542 (2003).

[39] K. H. Smith, E. Shero, A. Chizmeshya, and G. H. Wolf, The equation of state of polyamorphic germania glass: A two-domain description of the viscoelastic response, J. Chem. Phys. **102**, 6851 (1995).

[40] G. Lelong, L. Cormier, G. Ferlat, V. Giordano, G. S. Henderson, A. Shukla, and G. Calas, Evidence of fivefold-coordinated Ge atoms in amorphous GeO_2 under pressure using inelastic x-ray scattering, Phys. Rev. B **85**, 134202 (2012).

[41] O. B. Tsiok, V. V. Brazhkin, A. G. Lyapin, and L. G. Khvostantsev, Logarithmic Kinetics of the Amorphous-Amorphous Transformations in SiO_2 and GeO_2 Glasses Under High Pressure, Phys. Rev. Lett. **80**, 999 (1998).

[42] V. V. Brazhkin, Y. Katayama, K. Trachenko, O. B. Tsiok, A. G. Lyapin, E. Artacho, M. Dove, G. Ferlat, Y. Inamura, and H. Saitoh, Nature of the Structural Transformations in B_2O_3 Glass Under High Pressure, Phys. Rev. Lett. **101**, 035702 (2008).

[43] M. M. Koza, B. Geil, K. Winkel, C. Köhler, F. Czeschka, M. Scheuermann, H. Schober, and T. Hansen, Nature of Amorphous Polymorphism of Water, Phys. Rev. Lett. **94**, 125506 (2005).

[44] O. Mishima and Y. Suzuki, Propagation of the polyamorphic transition of ice and the liquid-liquid critical point, Nature (London) **419**, 599 (2002).